

Online Algorithms for Estimating Change Rates of Web Pages

Konstantin Avrachenkov¹, Kishor Patil¹, and Gudan Thoppe²

¹INRIA Sophia Antipolis, France 06902*

²Indian Institute of Science, Bengaluru, India 560012

Abstract

For providing quick and accurate search results, a search engine maintains a local snapshot of the entire web. And, to keep this local cache fresh, it employs a crawler for tracking changes across various web pages. It would have been ideal if the crawler managed to update the local snapshot as soon as a page changed on the web. However, finite bandwidth availability and server restrictions mean that there is a bound on how frequently the different pages can be crawled. This then brings forth the following optimisation problem: maximise the freshness of the local cache subject to the crawling frequency being within the prescribed bounds.

Recently, tractable algorithms have been proposed to solve this optimisation problem under different cost criteria. However, these assume the knowledge of exact page change rates, which is unrealistic in practice. We address this issue here. Specifically, we provide three novel schemes for online estimation of page change rates. All these schemes only need partial information about the page change process, i.e., they only need to know if the page has changed or not since the last crawl instance. Our first scheme is based on the law of large numbers, the second on the theory of stochastic approximation, while the third is an extension of the second and involves an additional momentum term. For all of these schemes, we prove convergence and, also, provide their convergence rates. As far as we know, the results concerning the third estimator is quite novel. Specifically, this is the first convergence type result for a stochastic approximation algorithm with momentum. Finally, we provide some numerical experiments (on real as well as synthetic data) to compare the performance of our proposed estimators with the existing ones (e.g., MLE).

1 Introduction

The world wide web is gigantic: it has a lot of interconnected information and both the information and the connections keep changing. However, irrespective of the challenges arising out of this, a user always expects a search engine to instantaneously provide accurate and up-to-date results. A search engine deals with this by maintaining a local cache of all the useful web pages and their links. As the freshness of this cache determines the quality of the search results, the search engine regularly updates it by employing a crawler (also referred to as a web spider or a web robot). The job of a crawler is (a) to discover new web pages; (b) to access various web pages at certain frequencies so as to determine if any changes have happened to the content since the last crawled instance; and (c) to update the local cache whenever there is a change. In this work we focus on tasks (b) and (c). To understand the detailed working of crawlers, see [2, 3, 4, 5, 6].

In general, a crawler has two constraints on how often it can access a page. The first one is due to limitations on the available bandwidth. The second one—also known as the politeness constraint—arises when a server imposes limits on the crawl frequency. The latter implies that the crawler can not access pages

*A shorter version [1] of this paper has appeared in the proceedings of ValueTools 2020. The novel contributions here include an additional online scheme (this is a stochastic approximation scheme with momentum) and additional experiments based on real data (Wikitraces).

*email: k.avrachenkov@inria.fr, kishor.patil@inria.fr, gudan.thoppe@gmail.com

on that server too often in a short amount of time. Such constraints cannot be ignored, since otherwise the server may forbid the crawler from all future accesses. In summary, to identify the ideal rates for crawling different web pages, a search engine needs to solve the following optimisation problem: Maximise the freshness of the local database subject to constraints on the crawling frequency.

In the early variants of this problem, the freshness of each page was assumed to be equally important [7, 6]. In such cases, experimental evidence somewhat surprisingly shows that the uniform policy—crawl all pages at the same frequency irrespective of their change rates—is more or less the optimal crawling strategy. Starting from the pioneering work in [8], however, the freshness definition was modified to include different weights for different pages depending on their importance, e.g., represented as the frequency of requests for the pages. The motivation for this change was the fact that only a finite number of pages can be crawled in any given time frame. Hence, to improve the utility of the local database, important pages should be kept as fresh as possible. Not surprisingly, under this new definition, the optimal crawling policy does indeed depend on the page change rates.

The above observation was numerically demonstrated first in [8] for a setup with a small number of pages. A more rigorous derivation of this fact was recently given in the path breaking paper [9]. In fact, this work also provides a near-linear time algorithm to find a near-optimal solution. A major concern for this algorithm is that it needs to know the actual values of the page change rates. However, in practice, these values are not known in advance and, instead, have to be estimated.

A separate study [10, 11] provides a Whittle index based dynamic programming approach to optimise the schedule of a web crawler. In that context, the page/catalogue freshness estimate also influences the optimal crawling policy and it also requires the good estimation of actual page change rates.

This work, which is an extended version of [1], is mainly motivated by the work from Azar et al. [9]. Our main contributions here can be summarised as follows. We propose three novel approaches for online estimation of the actual page change rates. The first is based on the Law of Large Numbers (LLN), the second is based on the Stochastic Approximation (SA) principles, while the third one is an extension of the second with an additional momentum term. Next, we theoretically show that all these estimators almost surely (a.s.) converge to the actual change rate values; thus, all our estimators are asymptotically consistent. To the best of our knowledge, the result concerning the third estimator is the first to show convergence of a stochastic approximation algorithm with momentum. We also rigorously derive the convergence rates of the first two estimators in the expected error sense. Based on the existing literature, we also provide a loose guess on the convergence rate of the third estimator. Finally, we provide numerical simulations to compare the performance of our online schemes to each other and also to that of the (offline) MLE estimator. Our experiments are based on both real (Wikipedia traces) as well as synthetic data sets. In one of our experiments, we also verify our modelling assumption that the page change process is a Poisson point process.

The rest of this paper is organised as follows. The next section provides a formal summary of this work in terms of the setup, goals, and key contributions. It also gives explicit update rules for all of our online schemes. In Section 3, we formally analyse their convergence and the rates of convergence. The numerical experiments discussed above are given in Section 4. Then, in Section 5, we provide some motivation on how one can use our estimates to find the optimal crawling rates. Finally, we conclude in Section 6 with some future directions.

2 Setup, Goal, and Key Contributions

The three topics are individually described below.

Setup: Without loss of generality, we work with a single web page. We presume that the actual times at which this page changes is a time-homogeneous Poisson point process in $[0, \infty)$ with a constant but unknown rate Δ . Independently of everything else, this page is crawled (accessed) at the random instances $\{t_k\}_{k \geq 0} \subset [0, \infty)$, where $t_0 = 0$ and the inter-arrival times, i.e., $\{t_k - t_{k-1}\}_{k \geq 1}$, are IID exponential random variables with a known rate p . Thus, the times at which this page is crawled is also a time-homogeneous Poisson point process but with rate p . At time instance t_k , we get to know if the page got modified or not in

the interval $(t_{k-1}, t_k]$, i.e., we can access the value of the indicator

$$I_k := \begin{cases} 1, & \text{if the page got modified in } (t_{k-1}, t_k], \\ 0, & \text{otherwise.} \end{cases}$$

The above assumptions are standard in the crawling literature, nevertheless, we now provide a quick justification for the same. Our assumption that the page change process is a Poisson point process is based on the experiments reported in [12, 13, 14]. Nevertheless, we also verify this assumption on a randomly selected page from frequently edited Wikipedia pages. We extract the complete history of this web page (exact time and date of a change) for a period of five months (April 01, 2020 to August 31, 2020). From the available history, we calculate the inter-arrival time of the page change process and plot Q-Q plot. We were indeed able to observe that the set of quantiles for real data matches linearly with the quantiles of exponential distribution; more details are present in the Section 4. Some generalised models for the page change process have also been considered in the literature [15, 16]; however, we do not pursue them here. Separately, our assumption on $\{I_k\}$ is based on the fact that a crawler can only access incomplete knowledge about the page change process. In particular, a crawler does not know when and how many times a page has changed between two crawling instances. Instead, all it can track is the status of a page at each crawling instance and know if it has changed or not with respect to the previous access. Sometimes, it is possible to also know the time at which the page was last modified [3, 17], but we do not consider this case here.

Goal: Develop online algorithms for estimating Δ in the above setup. The motivation for doing this is that such estimates can then be used to estimate the optimal crawling rates [9, 18]; see Section 5 for more details on this.

Key Contributions: We present three online methods for estimating the page change rate Δ . The first is based on the law of large numbers, while the second and third are based on the theory of stochastic approximation with the third one having an additional momentum component. If $\{x_k\}$, $\{y_k\}$, and $\{z_k\}$, denote the iterates of these three methods, respectively, then their update rules are as shown below.

- *LLN Estimator:* For $k \geq 1$,

$$x_k = p\hat{I}_k / (k + \alpha_k - \hat{I}_k). \quad (1)$$

Here, $\hat{I}_k = \sum_{j=1}^k I_j$; hence, $\hat{I}_k = \hat{I}_{k-1} + I_k$. And, $\{\alpha_k\}$ is any positive sequence satisfying the conditions in Theorem 1; e.g., $\{\alpha_k\}$ could be $\{1\}$, $\{\log k\}$, or $\{\sqrt{k}\}$.

- *SA Estimator:* For $k \geq 0$ and some initial value y_0 ,

$$y_{k+1} = y_k + \eta_k [I_{k+1}(y_k + p) - y_k]. \quad (2)$$

Here, $\{\eta_k\}$ is any stepsize sequence that satisfies the conditions in Theorem 2. For example, $\{\eta_k\}$ could be $\{1/(k+1)^\eta\}$ for some $\eta \in (0, 1]$.

- *SAM Estimator (SA Estimator with Momentum):* For $k \geq 0$ and some initial values z_0, z_{-1} ,

$$z_{k+1} = z_k + \eta_k [I_{k+1}(z_k + p) - z_k] + \zeta_k (z_k - z_{k-1}). \quad (3)$$

Here, $\{\eta_k\}$ and $\{\zeta_k\}$ are any stepsize sequences that satisfy the conditions given in Theorem 3. For example, pick a $\beta \in (1/2, 1]$ and let $\beta_k = 1/(k+1)^\beta$. Then, $\{\eta_k\}$ and $\{\zeta_k\}$ could be $\{1/(k+1)^\eta\}$ and $\{(\beta_k - \omega\eta_k)/(\beta_{k-1})\}$, respectively, where $\omega > 0$ is some constant and $\beta < \eta \leq 2\beta$. While we do not show it, we conjecture that one can also pick $\beta \in (0, 1/2]$ and then choose η so that $\beta < \eta \leq 2\beta$. Note that if $\beta = \eta$ and $\omega = 1$, then the asymptotic behaviour of (3) will resemble that of (2); this is because $\lim_{k \rightarrow \infty} \zeta_k = 0$ then.

We call these methods online because the estimates can be updated on the fly as and when a new observation I_k becomes available. This contrasts the MLE estimator in which one needs to start the calculation from scratch each time a new data point arrives. Also, unlike MLE, our estimators are never unstable; see Section 3.4 for the details.

Our main results include the following. We show that all our three estimators, i.e., x_k , y_k , and z_k , converge to Δ a.s. Further, we show that

1. $\mathbb{E}\|x_k - \Delta\| = O\left(\max\{k^{-1/2}, \alpha_k/k\}\right)$, and
2. $\mathbb{E}\|y_k - \Delta\| = O(k^{-\eta/2})$ if $\eta_k = (k+1)^\eta$ with $\eta \in (0, 1)$.

Separately, based on existing literature [19, 20, 21], we conjecture that $\mathbb{E}\|z_k - \Delta\| = \tilde{O}(k^{-\beta/2})$, where \tilde{O} hides logarithmic terms. However, we believe that this estimate is not tight in our setup; see Remark 8.

Finally, we provide several numerical experiments based on real as well as synthetic data for judging the strength of our three proposed estimators.

3 Analysis of the Proposed Online Estimators

Here, we formally discuss the convergence and convergence rates of our three estimators. Thereafter, we compare their behaviours with the estimators that already exist in the literature—the Naive estimator, the MLE estimator, and the Moment Matching (MM) estimator [22].

3.1 LLN Estimator

Our first aim here is to obtain a formula for $\mathbb{E}[I_1]$. We shall use this later to motivate the form of our LLN estimator.

Let $\tau_1 = t_1 - t_0 = t_1$, where the second equality holds since $t_0 = 0$. Then, as per our assumptions in Section 2, τ_1 is an exponential random variable with rate p . Also, $\mathbb{E}[I_1|\tau_1 = \tau] = 1 - \exp(-\Delta\tau)$. Hence,

$$\mathbb{E}[I_1] = \Delta/(\Delta + p). \quad (4)$$

This gives the desired formula for $\mathbb{E}[I_1]$.

From this latter calculation, we have

$$\Delta = p\mathbb{E}[I_1]/(1 - \mathbb{E}[I_1]). \quad (5)$$

Separately, because $\{I_k\}$ is an IID sequence and $\mathbb{E}[I_1] \leq 1$, it follows from the strong law of large numbers that $\mathbb{E}[I_1] = \lim_{k \rightarrow \infty} \sum_{j=1}^k I_j/k$ a.s. Thus,

$$\Delta = p \frac{\lim_{k \rightarrow \infty} \sum_{j=1}^k I_j/k}{1 - \lim_{k \rightarrow \infty} \sum_{j=1}^k I_j/k} \quad \text{a.s.}$$

Consequently, a natural estimator for Δ is

$$x'_k = p \frac{\sum_{j=1}^k I_j/k}{1 - \sum_{j=1}^k I_j/k} = p \frac{\hat{I}_k}{k - \hat{I}_k}, \quad (6)$$

where \hat{I}_k is as defined below (1).

Unfortunately, the above estimator faces an instability issue, i.e., $x'_k = \infty$ when I_1, \dots, I_k are all 1. To fix this, one can add a non-zero term in the denominator. The different choices then gives rise to the LLN estimator defined in (1).

The following result discusses the convergence and convergence rate of this estimator.

Theorem 1. Consider the estimator given in (1) for some positive sequence $\{\alpha_k\}$.

1. If $\lim_{k \rightarrow \infty} \alpha_k/k = 0$, then $\lim_{k \rightarrow \infty} x_k = \Delta$ a.s.

2. Additionally, if $\lim_{k \rightarrow \infty} \log(k/\alpha_k)/k = 0$, then

$$\mathbb{E}|x_k - \Delta| = O\left(\max\left\{k^{-1/2}, \alpha_k/k\right\}\right).$$

Proof. Let $\mu = \mathbb{E}[I_1]$, $\bar{I}_k = \hat{I}_k/k$, and $\bar{\alpha}_k = \alpha_k/k$. Then, observe that (1) can be rewritten as $x_k = p\bar{I}_k/(1 + \bar{\alpha}_k - \bar{I}_k)$. Now, $\lim_{k \rightarrow \infty} \bar{I}_k = \mu$ a.s. and $\lim_{k \rightarrow \infty} \bar{\alpha}_k = 0$; the first claim holds due to the strong law of large numbers, while the second one is true due to our assumption. Statement 1. is now easy to see.

We now derive Statement 2. From (5), we have

$$|x_k - \Delta| = \left| x_k - p \frac{\mu}{1 - \mu} \right| \leq p(A_k + B_k),$$

where

$$A_k = \left| \frac{\bar{I}_k}{\bar{\alpha}_k + 1 - \bar{I}_k} - \frac{\mu}{\bar{\alpha}_k + 1 - \mu} \right| \quad \text{and} \quad B_k = \left| \frac{\mu}{\bar{\alpha}_k + 1 - \mu} - \frac{\mu}{1 - \mu} \right|.$$

Since $\alpha_k > 0$ and, hence, $\bar{\alpha}_k > 0$, it follows that

$$B_k = \bar{\alpha}_k \frac{\mu}{(1 - \mu)(\bar{\alpha}_k + (1 - \mu))} \leq \bar{\alpha}_k \frac{\mu}{(1 - \mu)^2}.$$

Similarly,

$$A_k \leq \left(\frac{1 + \bar{\alpha}_k}{1 - \mu} \right) \left(\frac{|\bar{I}_k - \mu|}{\bar{\alpha}_k + 1 - \bar{I}_k} \right).$$

It is now easy to see that $\mathbb{E}[B_k] = O(\bar{\alpha}_k)$. The rest of our arguments concern how fast $\mathbb{E}[A_k]$ decays to 0.

Let $\{\delta_k\}$ be a deterministic sequence that is both non-negative and decays to 0. We will describe how to pick this later. Let k be such that $(1 + \delta_k)\mu < 1$. Then,

$$\mathbb{E} \left[\frac{|\bar{I}_k - \mu|}{\bar{\alpha}_k + 1 - \bar{I}_k} \right] \leq \mathbb{E}[C_k] + \mathbb{E}[D_k],$$

where

$$C_k = \frac{|\bar{I}_k - \mu|}{\bar{\alpha}_k + 1 - \bar{I}_k} \mathbf{1}\{\bar{I}_k - \mu \leq \delta_k \mu\},$$

and

$$D_k = \frac{|\bar{I}_k - \mu|}{\bar{\alpha}_k + 1 - \bar{I}_k} \mathbf{1}\{\bar{I}_k - \mu \geq \delta_k \mu\}.$$

On the one hand,

$$\mathbb{E}[C_k] \leq \frac{\mathbb{E}|\bar{I}_k - \mu|}{\bar{\alpha}_k + 1 - (1 + \delta_k)\mu} \leq \frac{\sqrt{\text{Var}[I_1]}}{\sqrt{k}(\bar{\alpha}_k + 1 - (1 + \delta_k)\mu)}.$$

On the other hand, since $|\bar{I}_k - \mu| \leq 2$ and $1 - \bar{I}_k \geq 0$, it follows by applying the Chernoff bound that

$$\mathbb{E}[D_k] \leq \frac{2}{\bar{\alpha}_k} \Pr\{\bar{I}_k \geq (1 + \delta_k)\mu\} \leq \frac{2}{\bar{\alpha}_k} \exp(-k\delta_k^2\mu/3).$$

Now, pick $\{\delta_k\}$ so that $\delta_k^2 = 6 \log(1/\bar{\alpha}_k)/(k\mu) \vee 0$ for all $k \geq 1$. Notice that this choice is both non-negative and decays to 0 due to our assumptions on $\{\alpha_k\}$; thus, this is a valid choice. It is now easy to see that $\mathbb{E}[C_k] = O(1/\sqrt{k})$ and $\mathbb{E}[D_k] = O(\bar{\alpha}_k)$.

The desired result now follows. \square

3.2 SA Estimator

Let I denote a random variable with the same distribution as I_1 . Also, for $y \in \mathbb{R}$, let $H(y, I) = I(y + p) - y$. Next, define $h : \mathbb{R} \rightarrow \mathbb{R}$ using $h(y) := \mathbb{E}[H(y, I)]$. Observe that $h(y) = p(\Delta - y)/(\Delta + p)$; further, Δ is its unique zero. The theory of stochastic approximation then suggests using the update rule given in (2) for estimating Δ .

We now discuss the convergence and convergence rate of this algorithm.

Theorem 2. *Consider the estimator given in (2) for some positive stepsize sequence $\{\eta_k\}$.*

1. *Suppose that $\sum_{k=0}^{\infty} \eta_k = \infty$ and $\sum_{k=0}^{\infty} \eta_k^2 < \infty$. Then, $\lim_{k \rightarrow \infty} y_k = \Delta$ a.s.*
2. *Suppose that $\eta_k = 1/(k+1)^\eta$ for some constant $\eta \in (0, 1)$. Then,*

$$\mathbb{E}|y_k - \Delta| = O\left(k^{-\eta/2}\right).$$

Proof. For $k \geq 0$, consider the σ -field $\mathcal{F}_k := \sigma(y_j, I_j, j \leq k)$. Then, from (4) and the fact that $\{I_k\}$ is an IID sequence, we get

$$\mathbb{E}[I_{k+1}(y_k + p) - y_k | \mathcal{F}_k] = \frac{\Delta}{\Delta + p}(y_k + p) - y_k = h(y_k).$$

Hence, one can rewrite (2) as

$$y_{k+1} = y_k + \eta_k[h(y_k) + M_{k+1}], \quad (7)$$

where

$$\begin{aligned} M_{k+1} &= [I_{k+1}(y_k + p) - y_k] - h(y_k) \\ &= \left[I_{k+1} - \frac{\Delta}{\Delta + p} \right] (y_k + p). \end{aligned} \quad (8)$$

Since $\mathbb{E}[M_{k+1} | \mathcal{F}_k] = 0$ for all $k \geq 0$, $\{M_k\}$ is a martingale difference sequence. Consequently, (7) is a classical SA algorithm whose limiting ODE is

$$\dot{y}(t) = h(y(t)). \quad (9)$$

We now make use of Theorem 9 given in the Appendix to establish Statement 1. Accordingly, we verify the four conditions listed there. The stepsize Condition i.) directly holds due to our assumptions on $\{\eta_k\}$. With regards to Condition ii.), recall we have already established above that $\{M_k\}$ is a martingale difference sequence with respect to $\{\mathcal{F}_k\}$. The square-integrability condition holds since $|M_{k+1}| \leq |y_k| + p$ which, in turn, implies that $\mathbb{E}[|M_{k+1}|^2 | \mathcal{F}_k] \leq 2(p^2 \vee 1)(1 + |y_k|^2)$, as desired. Next, due to linearity, h is trivially Lipschitz continuous. Further, $h(y) = 0$ if and only if $y = \Delta$. This shows that Δ is the unique equilibrium point of (9). Now, because the coefficient of y in $h(y)$ is negative, it also follows that Δ is the unique globally asymptotically stable equilibrium of (9). This verifies Condition iii.). We finally consider Condition iv.) Let $h_\infty(y) := -yp/(\Delta + p)$. Then, clearly, $h_c \rightarrow h_\infty$ uniformly on compacts as $c \rightarrow \infty$. Furthermore, since the coefficient of y is negative in the definition of h_∞ , it is easy to see that the origin is the unique globally asymptotically stable equilibrium of the ODE $\dot{y}(t) = h_\infty(y(t))$, as required. Statement 1. now follows.

We now sketch a proof for Statement 2. First, note that

$$y_{k+1} - \Delta = (1 - a\eta_k)(y_k - \Delta) + \eta_k M_{k+1},$$

where $a = p/(\Delta + p)$. Now, since $\mathbb{E}[M_{k+1} | \mathcal{F}_k] = 0$, we have

$$\mathbb{E}[(y_{k+1} - \Delta)^2 | \mathcal{F}_k] = (1 - a\eta_k)^2 (y_k - \Delta)^2 + \eta_k^2 \mathbb{E}[M_{k+1}^2 | \mathcal{F}_k].$$

Recall that $\mathbb{E}[M_{k+1}^2 | \mathcal{F}_k] \leq C(1 + y_k^2)$ for some constant $C \geq 0$. By substituting this above and then repeating all the steps from the proof of [23, Theorem 3.1], it is not difficult to see that Statement 2 holds as well. \square

3.3 SA Estimator with Momentum

In simple words, our SAM estimator is the SA estimator discussed above with an additional momentum term. Simulations in Section 4 show that this simple modification results in a drastic improvement in performance.

We now discuss the convergence of the SAM estimator under the assumption that, for $k \geq 0$,

$$\zeta_k = \frac{\beta_k - \omega\eta_k}{\beta_{k-1}}, \quad (10)$$

where $\omega > 0$ is some constant and $\{\beta_k\}$ is some positive real sequence. By substituting (10) and letting $u_k = (z_k - z_{k-1})/\beta_{k-1}$, observe that the update rule in (3) can be rewritten as

$$u_{k+1} = u_k + \gamma_k [I_{k+1}(z_k + p_i) - z_k] - \omega\gamma_k u_k,$$

where $\gamma_k := \eta_k/\beta_k$.

For $k \geq 0$, let M_{k+1} be as in (8). Also, let \mathcal{F}_k denote the σ -field $\sigma(z_0, u_0, I_1, \dots, I_k)$. Clearly, $u_k, z_k \in \mathcal{F}_k$ and $\mathbb{E}[M_{k+1}|\mathcal{F}_k] = 0$. Hence, $\{M_k\}$ is again a martingale difference sequence with respect to the filtration $\{\mathcal{F}_k\}$. Furthermore, since $|M_{k+1}| \leq |z_k| + p$, we have

$$\mathbb{E}[|M_{k+1}|^2|\mathcal{F}_k] \leq 2(p^2 \vee 1)(1 + |z_k|^2). \quad (11)$$

As before, let $a = p/(\Delta + p)$. Also, let $b = \Delta p/(\Delta + p)$ and $\epsilon_k = u_{k+1} - u_k$ for $k \geq 0$. It is then easy to see that one can write down (3) in terms of the following two update rules:

$$u_{k+1} = u_k + \gamma_k [h(u_k, z_k) + M_{k+1}] \quad (12)$$

$$z_{k+1} = z_k + \beta_k [g(u_k, z_k) + \epsilon_k], \quad (13)$$

where $h : \mathbb{R}^2 \rightarrow \mathbb{R}$ and $g : \mathbb{R}^2 \rightarrow \mathbb{R}$ are the linear functions given by

$$h(u, z) = b - \omega u - a z \quad \text{and} \quad g(u, z) = u.$$

Theorem 3. *Consider the SAM estimator given in (3) with ζ_k of the form given in (10). Then $z_k \rightarrow \Delta$ a.s., if one of the following conditions holds true.*

1. One-timescale : $\sum_{k \geq 0} \beta_k = \infty$, $\sum_{k \geq 0} \beta_k^2 < \infty$, and $\beta_k = \gamma_k$.
2. Two-timescale: $\sum_{k \geq 0} \beta_k = \sum_{k \geq 0} \gamma_k = \infty$, $\sum_{k \geq 0} (\beta_k^2 + \gamma_k^2) < \infty$, and $\lim_{k \rightarrow \infty} \frac{\beta_k}{\gamma_k} = 0$.

Recall that $\gamma_k = \eta_k/\beta_k$.

We state a few remarks concerning this result before discussing its proof.

Remark 4. Examples of $\{\eta_k\}$ and $\{\beta_k\}$ sequences such that the above conditions are satisfied include the following.

- *One-timescale:* $\beta_k = 1/(k+1)^\beta$ with $\beta \in (1/2, 1]$ and $\eta_k = 1/(k+1)^\eta$ with $\eta = 2\beta$.
- *Two-timescale:* $\beta_k = 1/(k+1)^\beta$ with $\beta \in (1/2, 1]$ and $\eta_k = 1/(k+1)^\eta$ with $\beta < \eta < 2\beta$.

In either case, note that $\lim_{k \rightarrow \infty} \zeta_k = 1$.

Remark 5. The justification for the names given above for the two sets of conditions is as follows. Under the first set of conditions, the update rules in (12) and (13) indeed behave like a one-timescale stochastic approximation algorithm, i.e., both u_k and z_k move on the same timescale. On the other hand, under the second set of conditions, (12) and (13), it behaves like a two-timescale stochastic approximation algorithm. This is because β_k decays to 0 at a much faster rate than γ_k , in turn implying that the changes in $\{z_k\}$, i.e., $\{z_{k+1} - z_k\}$ are of a smaller magnitude than that in $\{u_k\}$.

Remark 6. In the spirit of the above remark, a natural question to consider is the following. Can one pick $\{\eta_k\}$ and $\{\beta_k\}$ so that $\eta_k/\beta_k^2 \rightarrow 0$ or, equivalently, $\gamma_k/\beta_k \rightarrow 0$? That is, can one pick the stepsizes so that u_k now becomes the slowly moving update relative to z_k ? The answer to this question seems to be no. This is because a couple of sufficient conditions needed to guarantee convergence (see Condition iii.) and iv.) in Theorem 11) no longer hold true for this new setup. Furthermore, simulations seem to suggest that the iterates, in fact, race to infinity.

Remark 7. Another question to consider is the following. Can one pick ω , $\{\beta_k\}$, and $\{\eta_k\}$ so that $\zeta_k \rightarrow \zeta$, where ζ is a constant in $(0, 1)$? In particular, can one choose $\omega = (1 - \zeta)$, $\beta_k = 1/(k + 1)^\beta$ with $\beta \in (1/2, 1]$ and then pick $\eta_k = 1/(k + 1)^\beta$ so that $\zeta_k \rightarrow \zeta$? The answer to this second question does not seem to be clear. This is because $\lim_{k \rightarrow \infty} \gamma_k$ would then equal 1. Consequently, again, one of the sufficient conditions to guarantee convergence (see condition i.) of Theorem 11) would no longer hold. However, simulations in this case do show some promise.

Remark 8. Based on the existing literature on convergence rates for one-timescale and two-timescale linear stochastic approximation [23, 19, 20, 21], one can conjecture that $\mathbb{E}|z_k - \Delta| = \tilde{O}(k^{-\beta/2})$ when $\{\beta_k\}$ and $\{\eta_k\}$ are chosen as described in Remark 4. This implies the optimal convergence rate would then again be $O(1/\sqrt{k})$, which matches the bound we have obtained in Theorem 2 for the SA estimator. However, we believe that this bound may not be tight in the case of the SAM estimator. This is because (13) lacks the martingale difference term and, typically, these are the kind of terms that dictate the convergence rates. Furthermore, simulations in Section 4 suggest that the SAM estimator always converges much faster than the SA estimator.

Proof of Theorem 3. We discuss the two cases one by one.

One-timescale Setup: In this case, the update rules given in (12) and (13) together form a one-timescale stochastic approximation algorithm. More specifically, if we let $v_k = \begin{bmatrix} u_k \\ z_k \end{bmatrix}$, then it follows that

$$v_{k+1} = v_k + \beta_k \left(H(v_k) + \begin{bmatrix} 0 \\ \epsilon_k \end{bmatrix} + \begin{bmatrix} M_{k+1} \\ 0 \end{bmatrix} \right), \quad (14)$$

where $H : \mathbb{R}^2 \rightarrow \mathbb{R}^2$ is the function defined by

$$H(v) = \begin{bmatrix} b \\ 0 \end{bmatrix} - \begin{bmatrix} \omega & a \\ -1 & 0 \end{bmatrix} v.$$

We now verify the four conditions listed in Theorem 9 and then make use of Proposition 10 (both given in the appendix) to show that $v_k \rightarrow \begin{bmatrix} 0 \\ \Delta \end{bmatrix} =: v_*$ a.s. This automatically implies $z_k \rightarrow \Delta$ a.s., which is what we need to prove.

Notice that the stepsize in (14) is β_k . Condition i.), therefore, trivially holds due to the assumptions made in Statement 1. Next, observe that the martingale difference term in (14) is the vector $\begin{bmatrix} M_{k+1} \\ 0 \end{bmatrix}$. This, along with (11) and the statements above it, shows that Condition ii.) is true as well.

With regards to Condition iii.), first note that H is trivially Lipschitz continuous due to the linearity of both its component functions. Next, since $\Delta = b/a$, we have that $H(v) = 0$ if and only if $v = v_*$. Furthermore, since a and ω are strictly positive, the real parts of the eigenvalues of the matrix in the definition of H are also positive. This can be seen from the following set of observations. To begin with, the associated characteristic equation of this matrix is

$$\lambda^2 - \lambda\omega + a = 0.$$

Hence, the roots are $\lambda = (\omega \pm \sqrt{\omega^2 - 4a})/2$. If $\omega^2 < 4a$, then the roots are complex valued; therefore, the real part of both these roots is $\omega/2$ which is clearly positive. On the other hand, if $\omega^2 \geq 4a$, then both the roots are real; further, the smallest of the two roots, i.e., $(\omega - \sqrt{\omega^2 - 4a})/2$, is strictly positive since $a > 0$. This shows that the negative of the matrix given in the definition of H is Hurwitz. Together, these observations

show that v_* is the unique globally asymptotically stable equilibrium of the ODE $\dot{v}(t) = H(v(t))$. This verifies Condition iii.).

Finally, let

$$H_\infty(v) = - \begin{bmatrix} \omega & a \\ -1 & 0 \end{bmatrix} v.$$

Then, it is easy to see that $H_c(v) \rightarrow H_\infty(v)$ uniformly on compact sets as $c \rightarrow \infty$. Also, $H_\infty(v) = 0$ if and only if $v = 0$. Furthermore, as shown before, the negative of the matrix in the definition of H_∞ is Hurwitz. This implies that the origin is the unique globally asymptotically stable equilibrium of the ODE $\dot{v}(t) = H_\infty(v)$. This verifies condition iv.).

It now remains to check if $\{\epsilon_k\}$ has the decaying behaviour described in Proposition 10. Towards this, since $|M_{k+1}| \leq (p + |z_k|)$, we have

$$\left\| \begin{bmatrix} 0 \\ \epsilon_k \end{bmatrix} \right\| \leq C' \gamma_k (1 + |u_k| + |z_k|) \leq C \gamma_k (1 + \|v_k\|)$$

for some constants $C, C' \geq 0$. Now, because γ_k decays to 0 as $k \rightarrow \infty$ due to the assumption in Statement 1., it follows that $\{\epsilon_k\}$ indeed has the desired behaviour.

This completes the proof in the one-timescale setup.

Two-timescale Setup: Since $\beta_k/\gamma_k \rightarrow 0$, one can perceive u_k to be changing on a faster timescale relative to y_k . Hence, the update rules in (12) and (13) can be viewed as a two-timescale stochastic approximation. We now verify the conditions listed in Theorem 11 and then use Proposition 12 (both given in the appendix) to conclude $z_k \rightarrow \Delta$ a.s.

Conditions i.) and ii.) trivially hold. Hence, we only focus on verifying Conditions iii.) and iv.) Because of linearity, h and g are trivially Lipschitz continuous. Next, let $\phi(z) = (b - az)/\omega$ for $z \in \mathbb{R}$. Clearly, ϕ is linear in z and, hence, Lipschitz continuous. Also, $h(\phi(z), z) = 0$. This, along with the fact that the sign in front of u in $h(u, z)$ is negative, shows that $\phi(z)$ is indeed the unique globally asymptotically stable equilibrium of the ODE $\dot{u}(t) = h(u(t), z)$. Next, observe that the ODE $\dot{z}(t) = g(\phi(z(t)), z(t))$ has the form $\dot{z}(t) = (b - az(t))/\omega$. Clearly, this ODE has Δ as its unique globally asymptotically stable equilibrium. This completes the verification of Condition iii.).

With regards to Condition iv.), first let h_∞ be the function defined by $h_\infty(u, z) = -\omega u - az$. Also, for $z \in \mathbb{R}$, let $\phi_\infty(z) = -az/\omega$. This function is linear in z and, hence, Lipschitz; also, $\phi_\infty(0) = 0$. Then, on the one hand, $h_c \rightarrow h_\infty$ uniformly on compacts as $c \rightarrow \infty$ and, on the other hand, the ODE $\dot{u}(t) = h_\infty(u(t), z)$ indeed has $\phi_\infty(z)$ as its unique globally asymptotically stable equilibrium. Finally, for $z \in \mathbb{R}$, let $g_\infty(z) = -az/\omega$. Then, trivially, $g_c \rightarrow g_\infty$ uniformly on compacts, as $c \rightarrow \infty$. Further, $\dot{z}(t) = g_\infty(z(t)) = -az(t)/\omega$ which indeed has the origin as its unique globally asymptotically stable equilibrium. With this, we finish with verifying Condition iv.).

Now, as per Proposition 12, we need to show that $\{\epsilon_k\}$ is asymptotically negligible. However, this is indeed true since $|M_{k+1}| \leq (z_k + p)$ which implies $|\epsilon_k| \leq C \gamma_k (1 + |u_k| + |z_k|)$ for some constant $C \geq 0$, and the fact that $\gamma_k \rightarrow 0$.

This shows that $(u_k, z_k) \rightarrow (\phi(\Delta), \Delta) = (0, \Delta)$ a.s., as desired. \square

3.4 Comparison with Existing Estimators

As far as we know, there are three other approaches in the literature for estimating page change rates—the Naive estimator, the MLE estimator, and the MM estimator. The details about the first two estimators can be found in [17] while, for the third one, one can look at [22]. We now do a comparison, within the context of our setup, between these estimators and the ones that we have proposed.

The Naive estimator simply uses the average number of changes detected to approximate the rate at which a page changes. That is, if the sequence $\{w_k\}$ denotes the values of the Naive estimator then, in our setup, $w_k = p\hat{I}_k/k$, where \hat{I}_k is as defined below (1). The intuition behind this is the following. If τ_1 is as defined at the beginning of Section 3.1, then observe that $\mathbb{E}[N(\tau_1)] = \Delta/p$. Hence, the Naive estimator tries

to approximate $E[N(\tau_1)]$ with \hat{I}_k/k so that the previous relation can then be used for guessing the change rate.

Clearly, $E[w_k] = p\Delta/(\Delta + p) \neq \Delta$. Also, from the strong law of large numbers, $w_k \xrightarrow{a.s.} p\Delta/(\Delta + p) \neq \Delta$. Thus, this estimator is not consistent and is also biased. This is to be expected since this estimator does not account for all the changes that occur between two consecutive accesses.

Next, we look at the MLE estimator. Informally, this estimator identifies the parameter value that has the highest probability of producing the observed set of observations. In our setup, the value of the MLE estimator is obtained by solving the following equation for Δ :

$$\sum_{j=1}^k I_j \tau_j / (\exp(\Delta \tau_j) - 1) = \sum_{j=1}^k (1 - I_j) \tau_j, \quad (15)$$

where $\tau_k = t_k - t_{k-1}$ and $\{t_k\}$ is as defined in Section 2. The derivation of this relation is given in [17, Appendix C]. As mentioned in [17, Section 4], the above estimator is consistent.

Note that the MLE estimator makes actual use of the inter-arrival crawl times $\{\tau_k\}$ unlike our two estimators and also the Naive estimator. In this sense, it fully accounts for the randomness and available information in the crawling process. And, as we shall see in the numerical section, the quality of the estimate obtained via MLE improves rapidly in comparison to the Naive estimator as the sample size increases.

However, MLE suffers in two aspects— computational tractability and mathematical instability. Specifically, note that the MLE estimator lacks a closed form expression. Therefore, one has to solve (15) by using numerical methods such as the NewtonRaphson method, Fishers Scoring Method, etc. Unfortunately, using these ideas to solve (15) takes more and more time as the number of samples grow. Also note that, under the above solution ideas, the MLE estimator works in an offline fashion. In that, each time we get a new observation, (15) needs to be solved afresh. This is because there is no easy way to efficiently reuse the calculations from one iteration into the next; note that the defining equation (15) changes in a significant and nontrivial way from one iteration to another.

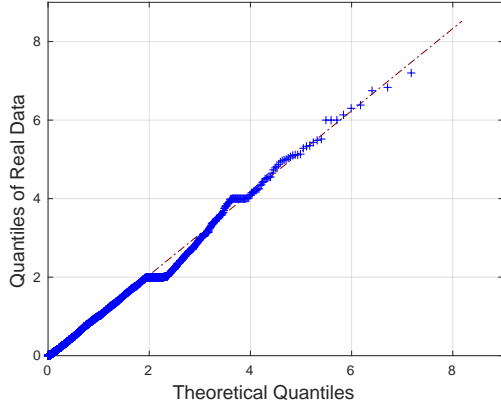
Besides the complexity, the MLE estimator is also unstable in two situations. One, when no changes have been detected ($I_j = 0, \forall k \in \{1, \dots, k\}$), and the other, when all the accesses detect a change ($I_j = 1, \forall k \in \{1, \dots, k\}$). In the first setting, no solution exists; in the second setting, the solution is ∞ . One simple strategy to avoid these instability issues is to clip the estimate to some pre-defined range whenever one of bad observation instances occur.

Finally, let us discuss the MM estimator. Here, one looks at the fraction of times no changes were detected during page accesses and then, using a moment matching method, tries to approximate the actual page change rate. In our context, the value of this estimator is obtained by solving $\sum_{j=1}^k (1 - I_j) = \sum_{j=1}^k e^{-\Delta \tau_j}$ for Δ . The details of this equation are given in [22, Section 4]. While the MM idea is indeed simpler than MLE, the associated estimation process continues to suffer from similar instability and computational issues like the ones discussed above.

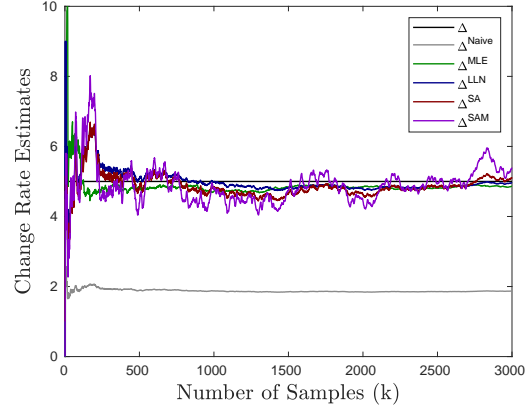
We emphasise that none of our estimators suffer from any of the issues mentioned above. In particular, all of our estimators are online and have a significantly simple update rule; thus, improving the estimate whenever a new data point arrives is extremely easy. Moreover, all of them are stable, i.e., the estimated values will almost surely be finite. More importantly, the performance of our estimators is comparable to that of MLE. This can be seen from the numerical experiments in Section 4.

4 Numerical Results

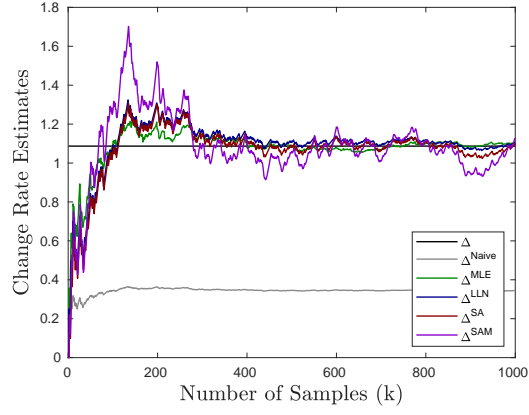
Here, we demonstrate the strength of our estimators using three different experiments. The first one involves real data based on Wikipedia traces. On the one hand, we use this experiment to provide a validation of our model assumption that the page change process is a stationary Poisson point process. On the other hand, we use it to demonstrate that the estimation quality of our online estimators is comparable to that of the offline MLE estimator. In the second experiment, using synthetic data, we study the impact of Δ and p on our three estimators. In the third experiment, we similarly study how the choice of $\{\alpha_k\}$, $\{\eta_k\}$ and $\{\beta_k\}$ influences the performance.



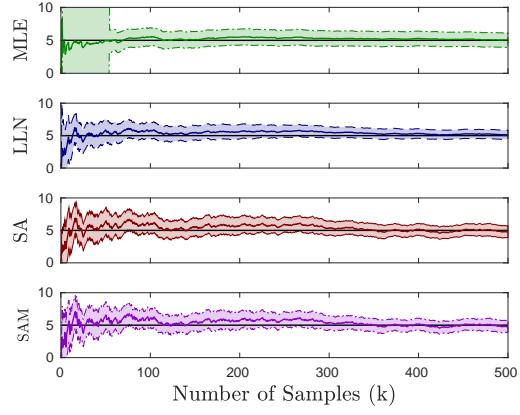
(a) Q-Q Plot: Real Data versus exponential distribution



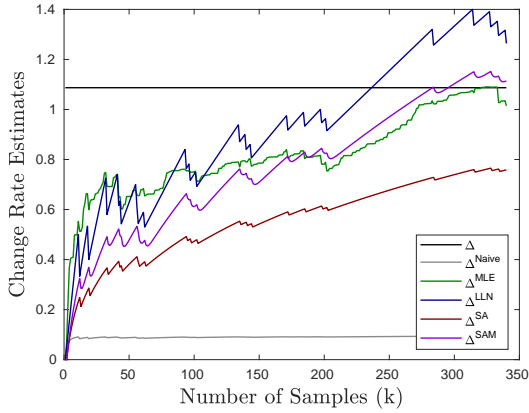
(a) Performance of single trajectories



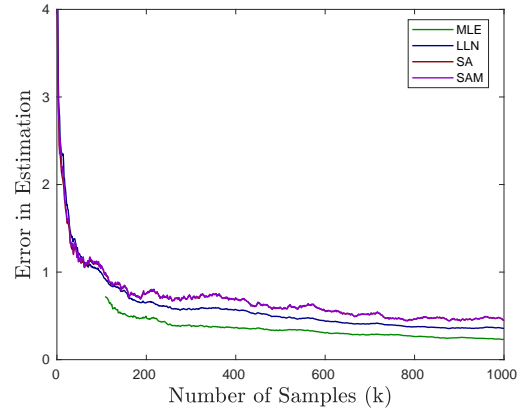
(b) $\Delta = 1.10$, $p = 0.5$



(b) 95% Confidence interval



(c) $\Delta = 1.10$, $p = 0.1$



(c) Root mean square error

Figure 1: Different Estimators: Real Data

Figure 2: Synthetic data: $\Delta = 5$, $p = 3$.

4.1 Performance on Real Data (Expt. 1)

As mentioned before, our goal here is provide a validation for our model as well as to compare the performance of the different estimators on real data.

To generate the data set, we used Wikipedia traces which are openly available on the web. In particular, we looked at the list of frequently edited pages on Wikipedia and then randomly selected one page. The title of the page we chose was ‘Template talk: Did you know’. Next, we extracted the timestamps at which this page was edited over the last five months (April 01, 2020 to August 31, 2020). We found that this page had changed 4043 times during this period. From the available history, we then calculated the inter-update times of the page change process. The average of these values turned out to be $\Delta = 1.1098$.

Using a Q-Q plot, we then compared the distribution of the collected data to that of an exponential distribution with rate parameter equal to this Δ value. That is, we used a scatterplot to compare the quantiles of the given data to that of the exponential distribution with rate 1.1098. The result is given in Fig. 1(a). Notice that the points roughly fall on a straight line and, more importantly, this line is very close to the 45° diagonal. This implies that both the sets of quantiles come from the same distribution, thereby confirming that the collected inter-update times indeed follow an exponential distribution whose rate is close to Δ . Equivalently, this implies that the update times come from a Poisson point process with rate parameter close to Δ .

Having verified our assumption, we now compare five different page rate estimators: Naive, MLE, LLN, SA, and SAM. Their performances are given in Fig 1(b) and Fig 1(c).

The procedure we adopted to obtain these plots was as follows. Unless specified, the notations are as in Section 2. Recall that we had access to the actual timestamps at which this Wikipedia page was changed. Keeping this in mind, we artificially generated the crawl instances of this page. These times were sampled from a Poisson point process with rate $p = 0.5$ for Fig 1(b) and with $p = 0.1$ for Fig 1(c). We then checked if the page had changed or not between each of the successive crawling instances. This then generated the values of the indicator sequence $\{I_k\}$. For $p = 0.5$, the length of this sequence was 1723 while, for $p = 0.1$, this length turned out to be 340. Using these I_k , p , and inter-update time lengths, we then used the five different estimators mentioned above to find Δ . This gave rise to the trajectories shown in Fig 1(b) and Fig 1(c). Note that the depicted trajectories correspond to exactly one run of each estimator. The trajectory of the estimates obtained by the SA estimator is labelled Δ^{SA} , etc. The stepsizes chosen for our different estimators are as follows. For our LLN estimator, we had set $\alpha_k \equiv 1$ and, for the SA estimator, we had used $\eta_k = (k + 1)^{-\eta}$ with $\eta = 0.75$. In case of the SAM estimator, we had set η_k as above, $\beta_k = (k + 1)^{-\beta}$ with $\beta = 0.6$ and $\omega = 1$. (Recall that, in the SAM estimator, the main stepsize is η_k while the stepsize multiplying the momentum term has the form $\zeta_k = (\beta_k - \omega\eta_k)/\beta_{k-1}$).

We now summarise our findings. In Fig 1(b), we observe that performances of the MLE, LLN, SA and SAM estimators are comparable to each other and all of them outperform the Naive estimator. This last observation is not at all surprising since the Naive estimator completely ignores the changes missed between two successive crawling instances. In contrast to this, we observe that the estimators behave somewhat differently in Fig 1(c). Recall that the crawling frequency here is 0.1, which is quite small compared with the value 0.5 that was chosen before. We notice that SAM and MLE estimators perform better than SA and LLN estimators in this scenario.

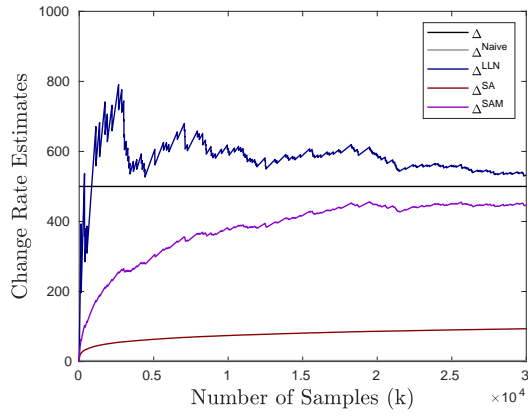
4.2 Comparison of Estimation Quality Using Synthetic Data (Expt. 2)

Throughout this experiment, we work with synthetic data.

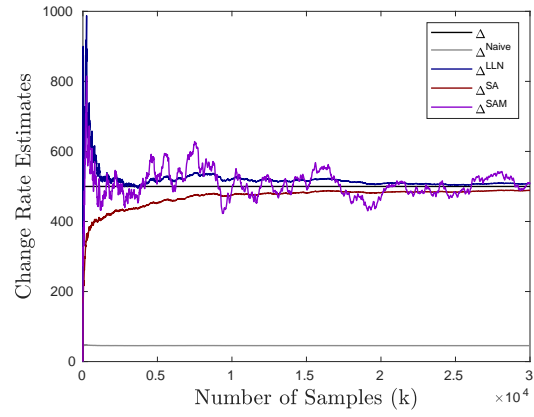
4.2.1 Sample Variance and Root Mean Squared Error

Our goal here is to study the sample variance and root mean squared error of the estimates obtained from multiple runs of the different estimators. The output is given in Fig. 2.

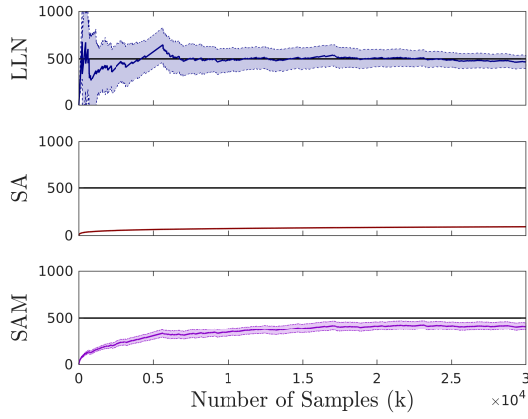
The data for this experiment is generated as follows. To begin with, we imagine there is only one page. We then sample points from two different stationary Poisson point processes, one with parameter $\Delta = 5$ and the other with parameter $p = 3$. We treat the samples from the first process as the times at which this page



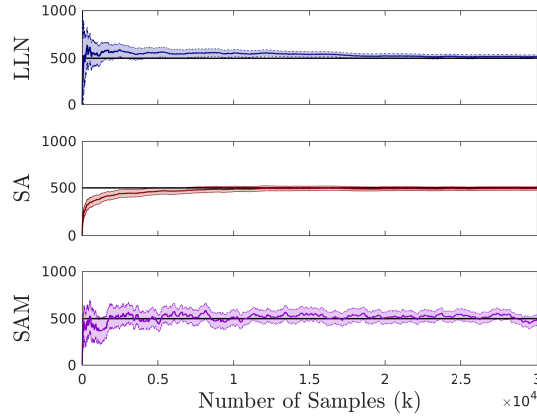
(a) Performance of single trajectories



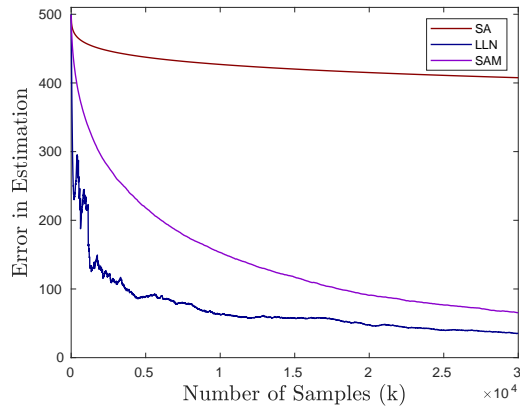
(a) Performance of single trajectories



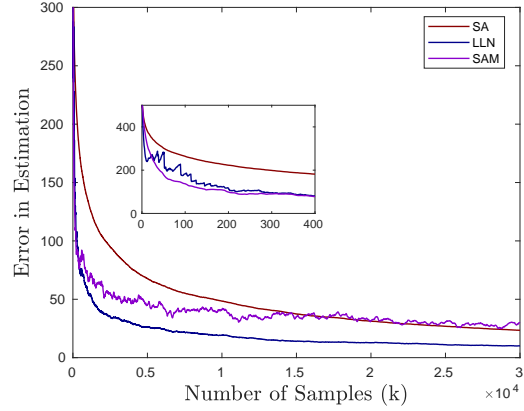
(b) 95% Confidence interval



(b) 95% Confidence interval



(c) Root mean square error



(c) Root mean square error

Figure 3: Synthetic data: $\Delta = 500$, $p = 3$.

Figure 4: Synthetic data: $\Delta = 500$, $p = 50$.

changes, and the samples from the second process as the times at which this page is crawled. We then check if the page has changed or not between two successive page accesses. This is then used to generate the values of the indicator sequence $\{I_k\}$.

We now give $\{I_k\}$, p , as well as the inter-access lengths as input to the five different estimators mentioned before. The stepsizes we use are as follows. For our LLN estimator, we set $\alpha_k \equiv 1$; for the SA estimator, we use $\eta_k = (k+1)^{-\eta}$ with $\eta = 0.75$; and, for the SAM estimator, we choose ζ_k as above, $\omega = 1$, and $\beta_k = (k+1)^{-\beta}$ with $\beta = 0.6$. Fig. 2(a) depicts one single run of each of the five estimators.

In Fig. 2(b) and Fig. 2(c), the parameter values are exactly the same as in Fig. 2(a). However, we now run the simulation 100 times; the page change times and the page access times are generated afresh in each run. Fig. 2(b) depicts the 95% confidence interval of the obtained estimates, whereas Fig. 2(c) shows the root mean squared value of the difference between the estimated value and actual change rate of the page.

We now summarise our findings. Clearly, in each case, we observe that performances of the MLE, LLN, SA and SAM estimators are comparable to each other and all of them outperform the Naive estimator. The fact that the estimates from our approaches are close to that of the MLE estimator was indeed quite surprising to us. This is because, unlike MLE, our estimators completely ignore the actual lengths of the intervals between two accesses. Instead, they use p , which only accounts for the mean interval length. Note that the variance of the first few samples for MLE is very high. This may be due to the instability that MLE faces; see Section 3.4. Fig. 2(c) shows that the error in the MLE estimate decays faster as compared to others. We believe this is because the MLE also uses the actual interval lengths in its computation; thus, it uses more information about the crawling process than the other estimators.

While the plots do not show this, we once again draw attention to the fact that the time taken by each iteration in MLE rapidly grows as k increases. In contrast, our estimators take roughly the same amount of time for each iteration.

4.2.2 Impact of Δ and p on Performance

In the previous experiments, recall that our different estimators more or less behaved similarly. Our goal now is to vary the values of Δ and p and see if there are any major differences that crop up in their performances. Alongside, we also wish to see the usefulness of the momentum term used in the SAM estimator. The performances in two such interesting scenarios are shown in Fig. 3 and Fig. 4. Note that we no longer consider MLE on account of their impractical run times when the I_k sequence lengths are large.

In Fig. 3, $\Delta = 500$ and $p = 3$, which means the crawling frequency is quite low compared to the frequency at which the page is updated. On the other hand, in Fig. 4, $\Delta = 500$ and $p = 50$; thus, the crawling frequency now is relatively higher. The stepsizes for our different estimators are as follows. For the LLN estimator, we chose $\alpha_k \equiv 1$; for the SA estimator, we chose $\eta_k = (k+1)^{-\eta}$ with $\eta = 0.8$; and, for the SAM estimator, we chose η_k as before, $\omega = 1$ and $\beta_k = (k+1)^{-\beta}$ with $\beta = 0.5$.

Fig. 3(a) and Fig. 4(a) show one single trajectory of our estimators in the two scenarios. We observe that the LLN and SAM estimators perform quite well as compared to the SA estimator in both the scenarios; however, the latter catches up when the p value becomes higher. The impact of the momentum term can also be clearly seen in the low frequency crawling case. In this scenario, note that the crawler will more or less always detects a change. That is, the $\{I_k\}$ sequence will mostly consists of all 1s. In turn, this means that the SA estimator's update rule will almost always have the form $y_{k+1} = y_k + \eta_k p$.

We then run the simulation 100 times and plot the 95% confidence interval and root mean squared error of our different estimators in the two scenarios. This is shown in Fig. 3(b), 3(c), 4(b), and 4(c). We observe that variance for SA is relatively very low. This is because the SA estimator does not deviate too much from the update rule mentioned in the previous paragraph. The disadvantage, however, is that its estimates typically are quite far away from the actual change rate. Furthermore, this error decreases quite slowly. Another interesting observation from Fig. 3(b) and 3(c) is that the variance of LLN estimator is larger than that of SAM estimator, however, its error decays at much faster rate than that of the SAM estimator.

In Fig. 4, notice that performance of all our estimators improve. However, as shown in Fig. 4(b), the SAM estimator is more noisy now. Separately, the zoomed-in plot in 4(c) shows that the average error for the SAM estimator drops quite rapidly compared to others in the initial few iterations. However, this advantage

disappears after 400 iterations; then on the LLN estimator is much more stable.

4.3 Impact of Step Size Choices (Expt.3)

The theoretical results presented in Section 3 show that the convergence rate of LLN, SA, and SAM estimator is affected by the choice of $\{\alpha_k\}$, $\{\eta_k\}$, and $\{\zeta_k\}$ respectively. Figures 5 provide a numerical verification of the same. The details are as follows. We chose $\Delta = 500$ and $p = 10$. Notice that the page change rate is again very high, whereas the crawling frequency is relatively very low value. We then use the LLN estimator with three different choices of $\{\alpha_k\}$; these choices are shown in the Fig 5(a) itself. The LLN estimator with $\alpha_k = k^{0.75}$ has the worst performance. This behaviour matches the prediction made by Theorem 1. In Fig. 5(b), we again consider the same setup as above. However, this time we run the SA estimator with three different choices of $\{\eta_k\}$; the choices are given in the figure itself. We see that the performance for $\eta = 0.5$ is better than the other cases.

We now analyse the impact of varying $\{\eta_k\}$ and $\{\zeta_k\}$ on the performance of the SAM estimator. Let ζ_k be of form given in (10). Based on Remark 4, pick $\eta_k = (k+1)^{-\eta}$ and $\beta_k = (k+1)^{-\beta}$ with $\beta \in (1/2, 1]$ and $\beta < \eta < 2\beta$. In Fig. 5(c), we fix $\eta = 0.8$ and vary β ; these choices are shown in the figure itself. The SAM estimator with $\beta = 0.4$ reaches the limit very quickly, however, it is very noisy and keeps fluctuating around actual change rate. The fluctuations reduce as the value of β increases; however, larger values of β also slow down the rate at which the error decreases. We observe that the SAM estimator with $\beta = 0.6$ has the best performance. In Fig. 5(d), we fix $\beta = 0.4$ and vary η . It is clear from the figure that the performance of the SAM estimator remains more or less the same. This implies that the major factor that affects the performance of SAM estimator is the stepsize related to momentum term.

Practical Recommendations:

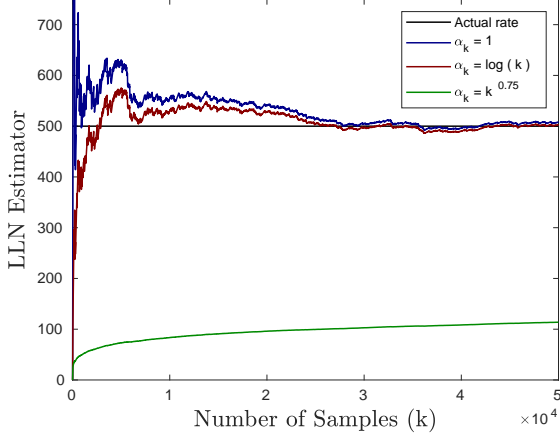
Here, we provide some recommendations on which estimator to use in practice. Our conclusions are based on what we have observed in the numerical experiments discussed in Section 4. We summarise them as follows.

- *High frequency crawling:* If the crawling frequency p is comparable to Δ , all estimators (LLN, SA, SAM and MLE) perform well except the Naive estimator. However, we do not recommend MLE as it is offline and very time-consuming. The examples that correspond to this scenario are depicted in Fig. 1(b) and Fig. 2.
- *Low frequency crawling:* There are two sub-cases depending on the value of p as compared to Δ .
 - Relatively very low p : The Naive estimator is very bad for this scenario as there will be several missed changes which will be unaccounted for. We recommend LLN or SAM estimator as they both outperform SA estimator; the example that corresponds to this scenario is depicted in Fig. 3. For similar reasons as in the previous case, we do not recommend the MLE estimator.
 - Relatively moderate p : The Naive estimator is again a bad choice here. Amongst the rest, we recommend the LLN estimator when several I_k values are available. Otherwise, one can use SAM or the MLE estimator; the offline nature of the MLE will be of concern here as well. The examples that corresponds to this scenario are depicted in Fig. 1(c) and Fig. 4.

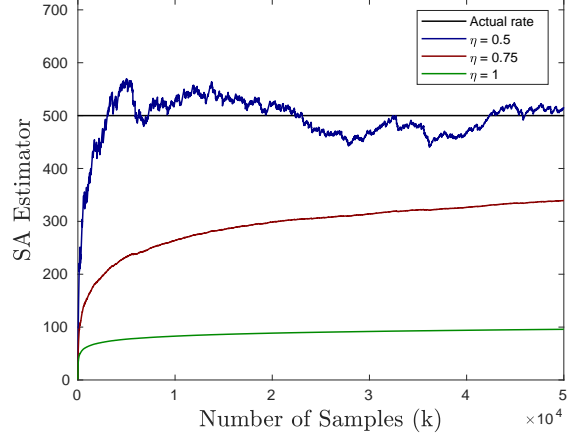
5 Motivation for Finding Page Change Rates

In this section, we discuss how our estimators can be used to find optimal crawling rates $\{p_i^*\}$ so that the overall freshness of the local cache

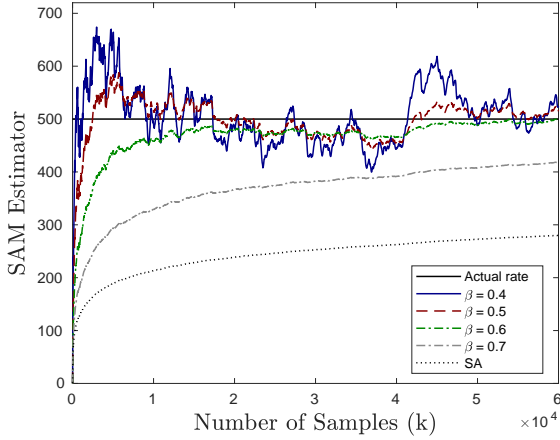
$$\lim_{T \rightarrow \infty} \mathbb{E} \left[\frac{1}{T} \int_0^T \left(\sum_{i=1}^N w_i \mathbf{1}\{\text{Fresh}(i, t)\} \right) dt \right] \quad (16)$$



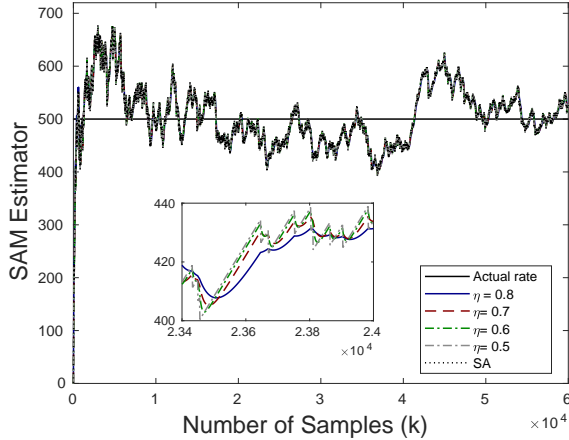
(a) LLN estimator for different $\{\alpha_k\}$ choices



(b) SA estimator with $\eta_k = (k+1)^{-\eta}$ for different η choices



(c) SAM estimator with $\eta = 0.8$ for different β_k choices



(d) SAM estimator with $\beta = 0.4$ for different η_k choices

Figure 5: Impact of $\{\alpha_k\}$, $\{\eta_k\}$ and $\{\zeta_k\}$ choices on Performance; $\Delta = 500$ and $p = 10$.

is maximised subject to $\sum_{i=1}^N p_i \leq B$. Here, $T > 0$ is some finite horizon, N is the number of pages, w_i denotes the importance of the i -th page, $B \geq 0$ is a bound on the overall crawling frequency, $1\{\cdot\}$ is the indicator, and $\text{Fresh}(i, t)$ is the event that page i is fresh at time t , i.e., the local copy matches the actual page.

Azar et al. [9] showed that maximising (16) under a bandwidth constraint for large enough T corresponds to maximising $F(p) = \sum_{i=0}^N (w_i p_i / (p_i + \Delta_i))$. Authors further provide an efficient algorithm with complexity $O(N \log N)$ to solve this equation. Note that this algorithm requires for Δ to be known in advance which can be estimated efficiently with any of the three schemes that we propose.

Separately, the recent work [18] along this direction view maximising freshness as minimising the harmonic staleness penalty related to every possible number of uncrawled changes. The associated problem now becomes minimising $\tilde{F}(p) = -\sum_{i=0}^N w_i \ln(p_i / (p_i + \Delta_i))$. All the algorithms provided in [18] also assume the known change rates, and authors use the MLE estimator to obtain them beforehand. Note that the

MLE estimator is offline and can be very time-consuming as the number of samples increases. Thus, one can replace it with any of our online estimators to obtain faster updates for page change rates.

6 Conclusion and Future Work

We have proposed three new online approaches for estimating the rate of change of web pages. All these estimators are computationally efficient in comparison to the MLE estimator. We first provide theoretical analysis on the convergence of our estimators and then provide numerical simulations to compare their performance with the existing estimators in the literature. From numerical experiments, we have verified that the proposed estimators perform significantly better than the Naive estimator and have extremely simple update rules which make them computationally attractive. We also provide important insights on which estimator one should use in practice.

The performance of both our estimators currently depend on the choice of $\{\alpha_k\}$, $\{\eta_k\}$, and $\{\zeta_k\}$ respectively. One aspect to analyse in the future would be to ask what would be the ideal choice for these sequences that would help attain the fastest convergence rate. Another interesting research direction is to combine the online estimation with dynamic optimisation.

Acknowledgement

This work is partly supported by ANSWER project PIA FSN2 (P15 9564-266178 \DOS0060094) and DST-Inria project "Machine Learning for Network Analytics" IFC/DST-Inria-2016-01/448. The authors would also like to thank A. Budhiraja for several useful discussions concerning Theorem 3.

References

- [1] Konstantin Avrachenkov, Kishor Patil, and Gagan Thoppe. Change rate estimation and optimal freshness in web page crawling. In *Proceedings of the 13th EAI International Conference on Performance Evaluation Methodologies and Tools*, pages 3–10, 2020.
- [2] Allan Heydon and Marc Najork. Mercator: A scalable, extensible web crawler. *World Wide Web*, 2(4):219–229, 1999.
- [3] Carlos Castillo. Effective web crawling. In *Acm sigir forum*, volume 39, pages 55–56, New York, NY, USA, 2005. Acm New York, NY, USA, Association for Computing Machinery.
- [4] Rahul Kumar, Anurag Jain, and Chetan Agrawal. A survey of web crawling algorithms. *Advances in vision computing: An international journal*, 3:1–7, 2016.
- [5] Christopher Olston, Marc Najork, et al. Web crawling. *Foundations and Trends® in Information Retrieval*, 4(3):175–246, 2010.
- [6] Jenny Edwards, Kevin McCurley, and John Tomlin. An adaptive model for optimizing performance of an incremental web crawler. In *Proceedings of the 10th International Conference on World Wide Web*, volume 8, page 106113, New York, NY, USA, 2001. Association for Computing Machinery.
- [7] Junghoo Cho and Hector Garcia-Molina. Synchronizing a database to improve freshness. *ACM sigmod record*, 29(2):117–128, 2000.
- [8] Junghoo Cho and Hector Garcia-Molina. Effective page refresh policies for web crawlers. *ACM Transactions on Database Systems (TODS)*, 28(4):390–426, 2003.
- [9] Yossi Azar, Eric Horvitz, Eyal Lubetzky, Yuval Peres, and Dafna Shahaf. Tractable near-optimal policies for crawling. *Proceedings of the National Academy of Sciences*, 115(32):8099–8103, 2018.

- [10] Konstantin E Avrachenkov and Vivek S Borkar. Whittle index policy for crawling ephemeral content. *IEEE Transactions on Control of Network Systems*, 5(1):446–455, 2016.
- [11] José Niño-Mora. A dynamic page-refresh index policy for web crawlers. In *Analytical and Stochastic Modeling Techniques and Applications*, pages 46–60, Cham, 2014. Springer International Publishing.
- [12] Brian E Brewington and George Cybenko. How dynamic is the web? *Computer Networks*, 33(1-6):257–276, 2000.
- [13] Brian E Brewington and George Cybenko. Keeping up with the changing web. *Computer*, 33(5):52–58, 2000.
- [14] Junghoo Cho and Hector Garcia-Molina. The evolution of the web and implications for an incremental crawler. In *26th International Conference on Very Large Databases*, pages 1–18, San Francisco, CA, USA, 2000. Morgan Kaufmann Publishers Inc.
- [15] Norman Matloff. Estimation of internet file-access/modification rates from indirect data. *ACM Transactions on Modeling and Computer Simulation (TOMACS)*, 15(3):233–253, 2005.
- [16] Sanasam Ranbir Singh. Estimating the rate of web page updates. In *Proc. International Joint Conferences on Artificial Intelligence*, pages 2874–2879, San Francisco, CA, USA, 2007. ACM.
- [17] Junghoo Cho and Hector Garcia-Molina. Estimating frequency of change. *ACM Transactions on Internet Technology (TOIT)*, 3(3):256–290, 2003.
- [18] Andrey Kolobov, Yuval Peres, Cheng Lu, and Eric J Horvitz. Staying up to date with online content changes using reinforcement learning for scheduling. In *Advances in Neural Information Processing Systems*, pages 581–591, 2019.
- [19] Gal Dalal, Gudan Thoppe, Balázs Szörényi, and Shie Mannor. Finite sample analysis of two-timescale stochastic approximation with applications to reinforcement learning. In *Conference On Learning Theory*, pages 1199–1233. PMLR, 2018.
- [20] Gal Dalal, Balázs Szörényi, and Gudan Thoppe. A tale of two-timescale reinforcement learning with the tightest finite-time bound. In *Thirty-Fourth AAAI Conference on Artificial Intelligence*, pages 3701–3708, San Francisco, CA, USA, 2020. AAAI Press.
- [21] Maxim Kaledin, Eric Moulines, Alexey Naumov, Vladislav Tadic, and Hoi-To Wai. Finite time analysis of linear two-timescale stochastic approximation with markovian noise. *arXiv preprint arXiv:2002.01268*, 2020.
- [22] Utkarsh Upadhyay, Robert Busa-Fekete, Wojciech Kotłowski, David Pal, and Balazs Szorenyi. Learning to crawl. In *Thirty-fourth AAAI Conference on Artificial Intelligence*, pages 8471–8478, New York, NY, USA, 2020. AAAI press.
- [23] Gal Dalal, Balázs Szörényi, Gudan Thoppe, and Shie Mannor. Finite sample analyses for td (0) with function approximation. In *Thirty-Second AAAI Conference on Artificial Intelligence*, pages 6144–6160, San Francisco, CA, USA, 2018. AAAI Press.
- [24] Vivek S Borkar. *Stochastic approximation: a dynamical systems viewpoint*, volume 48. Springer, India, 2009.
- [25] Chandrashekar Lakshminarayanan and Shalabh Bhatnagar. A stability criterion for two timescale stochastic approximation schemes. *Automatica*, 79:108–114, 2017.

A Convergence of Stochastic Approximation Algorithms

In this section, we discuss results from literature that provide sufficient conditions for convergence of both one-timescale and two-timescale stochastic approximation algorithms.

We begin by discussing the convergence of a generic one-timescale stochastic approximation algorithm. This result is obtained by combining [24, Chapter 2, Corollary 4,] and [24, Chapter 3, Theorem 7].

Theorem 9 (Convergence of One-timescale Stochastic Approximation [24]). *Consider the update rule*

$$y_{k+1} = y_k + \eta_k [h(y_k) + M_{k+1}],$$

where η_k is a positive scalar; $y_k, M_k \in \mathbb{R}^d$; and $h : \mathbb{R}^d \rightarrow \mathbb{R}^d$ is a deterministic function. Suppose the following conditions hold:

i.) $\sum_{k=0}^{\infty} \eta_k = \infty$ and $\sum_{k=0}^{\infty} \eta_k^2 < \infty$.

ii.) $\{M_k\}$ is a martingale difference sequence with respect to the increasing family of σ -fields

$$\mathcal{F}_k := \sigma(y_j, M_j, j \leq k), \quad k \geq 0.$$

That is, $\mathbb{E}[M_{k+1} | \mathcal{F}_k] = 0$ a.s., $k \geq 0$. Further, there is a constant $C \geq 0$ such that $\mathbb{E}[\|M_{k+1}\|^2 | \mathcal{F}_k] \leq C(1 + \|y_k\|^2)$ a.s. for all $k \geq 0$.

iii.) h is a globally Lipschitz continuous function. Further, the ODE $\dot{y}(t) = h(y(t))$ has an unique globally asymptotically stable equilibrium y_* .

iv.) There exists a continuous function $h_\infty : \mathbb{R}^d \rightarrow \mathbb{R}^d$ such that the functions $h_c(x) := h(cx)/c$, $c \geq 1$, satisfy $h_c \rightarrow h_\infty$ uniformly on compact sets as $c \rightarrow \infty$. Further, the ODE $\dot{y}(t) = h_\infty(y(t))$ has the origin as its unique globally asymptotically stable equilibrium.

Then, $y_k \rightarrow y_*$ a.s.

Often, stochastic approximation algorithms contain an additional perturbation term that is asymptotically negligible. The next result discusses convergence of such algorithms.

Proposition 10 (Convergence of Perturbed One-timescale Stochastic Approximation). *Consider the update rule*

$$y_{k+1} = y_k + \eta_k [h(y_k) + \epsilon_k + M_{k+1}],$$

where ϵ_k is an additional perturbation term while the other terms have the same meaning as in Theorem 9. Suppose that the four conditions listed in Theorem 9 hold true. Further, suppose $\|\epsilon_k\| \leq C\rho_k(1 + \|y_k\|)$ a.s. for $k \geq 0$, where C is a positive constant and $\{\rho_k\}$ is a sequence of positive scalars such that $\lim_{k \rightarrow \infty} \rho_k = 0$. Then, $y_k \rightarrow y_*$ a.s.

Proof. We only give a sketch of the proof since the arguments are more or less similar to the ones used to derive Theorem 9. As mentioned before, this latter result follows from [24, Chapter 2, Corollary 4] and [24, Chapter 3, Theorem 7]. We now briefly discuss how, even in the presence of the additional perturbation term, these two results continue to hold.

- [24, Chapter 2, Corollary 4]: This result follows from [24, Chapter 2, Theorem 2] which, in turn, follows from [24, Chapter 2, Lemma 1]. However, as shown in extension 3 in [24, pg. 17], this latter result goes through even in the presence of the perturbation term $\{\epsilon_k\}$. This is because ϵ_k is asymptotically negligible a.s. More specifically, observe that the sequence $\{y_k\}$ is a.s. bounded under assumption **(A4)** given on [24, pg. 17]. This implies that $\{\epsilon_k\}$ is a random bounded sequence which is $o(1)$ a.s.; the latter is true since $\rho_k \rightarrow 0$.

- [24, Chapter 3, Theorem 7]: The proof of this result is based on Lemmas 1 to 6 in [24, Chapter 3]. The first three of these lemmas concerns the behaviour of the solution trajectories of the limiting ODE $\dot{y}(t) = h_\infty(y(t))$. Since the perturbation term does not affect the definition of this limiting ODE in any way whatsoever, these three results continue to hold as before. Similarly, Lemma 5 in ibid is unchanged since it only concerns the convergence of the sum of martingale differences $\sum_k \eta_k \hat{M}_{k+1}$ (recall that the stepsize sequence in our update rule is η_k). With regards to the proof of Lemma 4 in ibid, observe that our update rule satisfies

$$\hat{y}(t(k+1)) = \hat{y}(t(k)) + \eta_k(h_{r(n)}(\hat{y}(t(k))) + \hat{\epsilon}_k + \hat{M}_{k+1}), \quad m(n) \leq k \leq m(n+1),$$

where $\hat{\epsilon}_k = \epsilon_k/r(n)$ while the other notations are analogous to the ones defined in [24, Chapter 3]. Because $\|\epsilon_k\| \leq C\rho_k(1 + \|y_k\|)$, $\rho_k \rightarrow 0$, and $r(n) \geq 1$, it follows that

$$\|\hat{\epsilon}_k\| \leq C_1(1 + \|\hat{y}(t(k))\|^2)$$

for some positive constant C_1 . Note that this is in similar spirit to (3.2.5) in ibid. It is then easy to see that the rest of the proof goes through as before. This shows that [24, Chapter 3, Lemma 4] continues to be true even in the presence of the the perturbation term. Using exactly the same bound for $\|\hat{\epsilon}_k\|$ obtained above, one can see that the arguments in the proof of Lemma 6 in ibid hold as well. Thus, [24, Chapter 3, Theorem 7] continues to hold, which is exactly what we wanted to establish.

The desired result now follows. \square

We next state a result that discusses the convergence of a generic two-timescale stochastic approximation algorithm. The proof of this result is based on [24, Chapter 6, Theorem 2] and [25, Theorem 10].

Theorem 11 (Convergence of Two-timescale Stochastic Approximation [24, 25]). *Consider the update rules*

$$\begin{aligned} u_{k+1} &= u_k + \gamma_k[h(u_k, z_k) + M_{k+1}^{(1)}], \\ z_{k+1} &= z_k + \beta_k[g(u_k, z_k) + M_{k+1}^{(2)}], \end{aligned}$$

where γ_k and β_k are positive scalars; $u_k, z_k, M_k^{(1)}, M_k^{(2)} \in \mathbb{R}^d$; and $h, g : \mathbb{R}^{2d} \rightarrow \mathbb{R}^d$ are two deterministic functions. Suppose the following conditions hold:

i.) $\sum_{k \geq 0} \gamma_k = \sum_{k \geq 0} \beta_k = \infty$, $\sum_{k \geq 0} (\gamma_k^2 + \beta_k^2) < \infty$, and $\lim_{k \rightarrow \infty} \frac{\beta_k}{\gamma_k} = 0$.

ii.) $\{M_k^{(1)}\}$ and $\{M_k^{(2)}\}$ are martingale difference sequences with respect to the increasing σ -fields

$$\mathcal{F}_k := \sigma(u_j, z_j, M_j^{(1)}, M_j^{(2)}, j \leq k), \quad k \geq 0.$$

Further, there exists a constant $C \geq 0$ such that $\mathbb{E}[\|M_{k+1}^{(i)}\|^2 | \mathcal{F}_k] \leq C(1 + \|u_k\|^2 + \|z_k\|^2)$ for $i = 1, 2$ and $k \geq 0$.

iii.) h and g are globally Lipschitz continuous functions. For each fixed z , the ODE $\dot{u}(t) = h(u(t), z)$ has a unique globally asymptotically stable equilibrium $\phi(z)$, where $\phi : \mathbb{R}^d \rightarrow \mathbb{R}^d$ is Lipschitz continuous. Further, the ODE $\dot{z}(t) = g(\phi(z(t)), z(t))$ has an unique globally asymptotically stable equilibrium z_* .

iv.) The functions $h_c(u, z) := h(cu, cz)/c$, $c \geq 1$, satisfy $h_c \rightarrow h_\infty$ as $c \rightarrow \infty$, uniformly on compacts for h_∞ . Also, for each fixed $z \in \mathbb{R}^d$, the limiting ODE $\dot{u}(t) = h_\infty(u(t), z)$ has a unique globally asymptotically stable equilibrium $\phi_\infty(z)$, where $\phi_\infty : \mathbb{R}^d \rightarrow \mathbb{R}^d$ is a Lipschitz map. Further, $\phi_\infty(0) = 0$. Separately, the functions $g_c(z) := g(c\phi_\infty(z), cz)/c$, $c \geq 1$, satisfy $g_c \rightarrow g_\infty$ as $c \rightarrow \infty$, uniformly on compacts for some g_∞ . Also, the limiting ODE $\dot{z}(t) = g_\infty(z(t))$ has the origin as its unique globally asymptotically stable equilibrium.

Then, $(u_k, z_k) \rightarrow (\phi(z_*), z_*)$ a.s.

The last and final result of this section concerns the convergence of two-timescale stochastic approximation with perturbation terms that are asymptotically negligible.

Proposition 12 (Convergence of Perturbed Two-timescale Stochastic Approximation). *Consider the update rules*

$$\begin{aligned} u_{k+1} &= u_k + \gamma_k [h(u_k, z_k) + \epsilon_k^{(1)} + M_{k+1}^{(1)}] \\ z_{k+1} &= z_k + \beta_k [g(u_k, z_k) + \epsilon_k^{(2)} + M_{k+1}^{(2)}], \end{aligned}$$

where $\epsilon_k^{(1)}, \epsilon_k^{(2)}$ are additional perturbation terms while the other terms have the same meaning as in Theorem 11. Suppose that the four conditions listed in Theorem 11 hold true. Further, suppose $\|\epsilon_k^{(i)}\| \leq C\rho_k^{(i)}(1 + \|u_k\| + \|z_k\|)$ a.s. for $k \geq 0$ and $i = 1, 2$, where C is a positive constant and $\{\rho_k^{(i)}\}$, $i = 1, 2$, are sequences of positive scalars such that $\lim_{k \rightarrow \infty} \rho_k^{(i)} = 0$. Then, $(u_k, z_k) \rightarrow (\phi(z_*), z_*)$ a.s.

Proof. As stated before, this result follows from [24, Chapter 6, Theorem 2] and [25, Theorem 10]. We now briefly discuss how these results continue to hold even in the presence of the perturbation terms $\epsilon_k^{(1)}$ and $\epsilon_k^{(2)}$.

- [24, Chapter 6, Theorem 2]: This result, as well as [24, Chapter 6, Lemma 1] on which it relies, are essentially proved by defining suitable one-timescale stochastic approximation algorithms and then using convergence results concerning the latter. In our situation, both these will have additional perturbation terms that are asymptotically negligible. Consequently, by arguing as in the third extension given in [24, pg. 27], it can be shown that the asymptotic behaviour of these two algorithms remains unchanged even in the perturbed setup. Therefore, it follows that the conclusions of [24, Chapter 6, Theorem 2] continue to hold as before.
- [25, Theorem 10]: This result is based on Lemmas 2 to 7 and Lemma 9 as well as Theorems 6 and 7 in *ibid.* Lemmas 2 to 5 in *ibid.* concern the limiting ODEs described in condition iv.) of Theorem 11 above. The definitions of these ODEs do not depend on the presence or absence of the perturbation terms. Therefore, the aforementioned four lemmas continue to hold as before. On the other hand, Lemmas 6 and 9 in *ibid.* rely on the results in Chapter 3 and Chapter 6 of [24]. As argued before, these results continue to hold even in the presence of perturbation terms and, consequently, so do Lemmas 6 and 9 in *ibid.* Finally, Theorems 8 and 10 in *ibid.* build upon these seven Lemmas. Therefore, they hold as well in the perturbed setup.

The desired result now follows. □